The Structure and Interactions of Human Apolipoprotein C-II in Dodecyl Phosphocholine[†,‡]

Christopher A. MacRaild, Geoffrey J. Howlett, and Paul R. Gooley*

Russell Grimwade School of Biochemistry and Molecular Biology, University of Melbourne, Parkville, Victoria 3010, Australia

Received January 26, 2004; Revised Manuscript Received May 3, 2004

ABSTRACT: The structure of human apolipoprotein C-II (apoC-II) in the presence of dodecyl phosphocholine (DPC) micelles has been investigated by NMR spectroscopy. The resulting structural information is compared to that available for apoC-II in the presence of sodium dodecyl sulfate, revealing a high level of overall similarity but several significant differences. These findings further our understandings of the structural basis for apoC-II function. The interactions of the protein with the detergent micelle are probed using intermolecular nuclear Overhauser effects (NOEs) and paramagnetic agents. These interactions are seen across almost the full length of apoC-II and show the periodicity expected for an amphipathic helix interacting with the amphipathic surface of the DPC micelle. Furthermore, we observe specific contacts between lysine residues of apoC-II and protons near the phosphate group of DPC, consistent with the predictions of the so-called "snorkel hypothesis" of the structural basis for the apolipoprotein/lipid interaction (Segrest, J. P., Jackson, R. L., Morrisett, J. D., and Gotto, A. M., Jr. (1974) A molecular theory of lipid−protein interactions in the plasma lipoproteins, *FEBS Lett 38*, 247−258.). These findings offer the most detailed structural information available for the interaction between an apolipoprotein and the phospholipids of the lipoprotein surface and provide the first direct structural support for the snorkel hypothesis.

Apolipoprotein C-II (apoC-II)[1] is a 79 residue exchangeable apolipoprotein (*1*) that plays an essential role in plasma lipid metabolism as the requisite cofactor for lipoprotein lipase (LpL) (*2*). LpL hydrolyses triacylglycerol during the metabolic remodeling of chylomicrons and very low-density lipoproteins, releasing fatty acids and glycerol to surrounding tissues for cellular uptake (*3*). Activation of LpL by apoC-II is determined by the capacity of apoC-II to bind LpL and stabilize a ternary complex with the lipoprotein substrate by means of the apoC-II lipid binding regions (*4*). ApoC-II binding may also induce a change in LpL conformation to expose the active site to substrate in a manner analogous to the interaction of pancreatic lipase with its protein cofactor, colipase (*5*). However in the absence of detailed structural information on the interaction of apoC-II with LpL or the lipoprotein particle, this model remains poorly defined and controversial.

As with the other exchangeable apolipoproteins, apoC-II binds reversibly to the polar lipid surface of plasma lipoprotein particles in vivo and associates with a range of natural and synthetic lipid surfaces in vitro with a concomitant change in secondary structure. Analysis of this conformational change and the amino acid sequence of the lipid binding regions involved has led to the generally accepted hypothesis that exchangeable apolipoproteins associate with lipid surfaces by means of class A_2 amphipathic helices predicted to be present in all members of the family (*6*). A_2 amphipathic helices are defined as α-helices in which the hydrophobic and hydrophilic residues are segregated onto opposite faces of the helix with positively charged residues at the interface between the polar and nonpolar faces and the negatively charged residues occupying the center of the polar face (*7*). It has been proposed that the affinity of these amphipathic helices for lipid surfaces is the result of a combination of hydrophobic interactions with the lipid tails and ionic interactions with phospholipid headgroups (*8*). Specifically it is proposed that the zwitterionic headgroups of phosphatidyl choline interact with this structural feature with the positively charged choline moiety interacting with the acidic residues in the center of the hydrophilic face, while the basic residues interact with the phosphate group. This hypothesis has been dubbed the "snorkel hypothesis", after the proposed conformation of the long basic side chains, reaching out of the hydrophobic region of the lipid monolayer to interact with the phospholipid headgroup.

A number of studies provide empirical support for the snorkel hypothesis. In particular, peptides designed to form class A_2 amphipathic helices associate strongly with phospholipid (*9*−*12*), while studies of apolipoprotein fragments show that lipid-binding functional domains are located in regions of predicted amphipathic helix (*13*−*19*). Several intact apolipoproteins and lipid-binding fragments show an increase in helical content on binding to lipid surfaces, suggesting that helix formation is favored by, or required for, lipid binding (*20*−*24*). Peptides in which the class A_2

[†] This work was funded by the National Health and Medical Research Council and the Australian Research Council. C.A.M. was the recipient of an Australian Postgraduate Award.

[‡] Atomic coordinates from this work have been submitted to the Protein Data Bank, PDB ID 1SOH. Chemical shift assignments have been submitted to BioMagResBank, accession no. 6143.

* To whom correspondence should be addressed. Phone +61 3 8344 5935; fax + 61 3 9347 7730; e-mail prg@unimelb.edu.au.

[1] Abbreviations: apoC-II, apolipoprotein C-II; LpL, lipoprotein lipase; SDS, sodium dodecyl sulfate; DPC, dodecyl phosphocholine.

10.1021/bi049817l CCC: $27.50
Published on Web 06/03/2004

motif is altered in various ways add significant support to the snorkel hypothesis. Peptides in which the conventional charge distribution is reversed show reduced lipid affinity (*10*, *25*, *26*), as do peptides in which the basic residues lysine and arginine are replaced with the much shorter side chain of homoaminoalanine (*27*).

Despite this abundance of indirect evidence, direct structural support for the snorkel hypothesis is lacking. Furthermore, a number of alternative models exist to explain the apolipoprotein/lipid interaction with at least one study suggesting that specific charge interactions between the protein and lipid do not have a role in lipid binding behavior but rather that the charge distribution on the helix results in favorable hydration properties of the protein/lipid complex (*28*). Furthermore, Gursky and colleagues have analyzed the thermal and chemical denaturation of apolipoproteins in the presence of lipid and suggest that lipoprotein stability has kinetic rather than thermodynamic origins (*29*−*31*). This conclusion casts into question the equilibrium thermodynamic approach used to analyze much of the previous work on apolipoprotein/lipid interactions. These ongoing controversies establish the need for a detailed understanding of apolipoprotein/lipid interactions in terms of high-resolution structure as well as thermodynamics.

Previously, we (*32*) and others (*33*) have used NMR techniques to characterize the structure of apoC-II in the presence of sodium dodecyl sulfate (SDS) micelles. These studies indicate a well-ordered helical conformation for the N-terminal half of the protein with the exception of the first 12 residues, which are unstructured. The C-terminal half is also helical, though some regions are less well constrained due to a lack of NOE data. While several features of these structural data are of interest in relation to the activation of LpL and the lipid-binding interactions of apoC-II, the lack of similarity between the SDS micelle and lipoprotein particles make the interpretation of these data problematic, particularly in terms of lipid interactions. In the present study, we have employed similar techniques to investigate the structure of apoC-II in the presence of dodecyl phosphocholine (DPC) micelles. In addition, we map specific protein/DPC contacts by means of intermolecular nuclear Overhauser effects (NOEs) and assess protein exposure to the aqueous and micellar environments by means of the effect of paramagnetic agents on the apoC-II backbone NMR resonances. DPC is a detergent that shares the phosphocholine headgroup with the phosphatidyl choline class of biological phospholipids, and by exploiting this similarity, we are able to infer details of the apoC-II/lipoprotein interaction.

MATERIALS AND METHODS

^{15}N-enriched human apoC-II was bacterially expressed and purified as described previously (*32*, *34*). Samples for NMR spectroscopy were prepared by solublizing lyophilized ^{15}N-apoC-II in 100% TFE and then evaporating the solvent under a flow of dry air. Final traces of TFE were removed under vacuum. Protein prepared in this manner was then dissolved in 500 μL of 85 mM DPC, 20 mM sodium acetate, 0.1% sodium azide, pH 5.0, and 50 μL of D_2O was added. The final protein concentration of samples for all experiments used for spectral assignment and collection of structural constraints was approximately 1.8 mM. These samples were stored at room temperature and found to be stable over several months, as monitored by ^{1}H,^{15}N heteronuclear single quantum coherence (HSQC) experiments.

NMR spectroscopy was performed on a Varian Inova 500 MHz NMR spectrometer equipped with a 5 mm ^{1}H, ^{13}C, ^{15}N single *z* axis gradient probe. Chemical shifts were referenced against 2,2-dimethyl-2-silapentane-5-sulfonic acid. All experiments were run at 30 °C. Typical acquisition parameters were as follows: two-dimensional ^{1}H,^{15}N HSQC spectra (*35*) were obtained using a spectral width of 6255.4 Hz and 1024 complex points in the ^{1}H dimension and a spectral width of 1200 Hz in the ^{15}N dimension with 128 t_1 increments. ^{1}H,^{15}N nuclear Overhauser effect spectroscopy (NOESY)−HSQC and total correlation spectroscopy (TOCSY)−HSQC spectra (*36*−*38*) were acquired with spectral widths of 5599.9, 5000.0, and 1350.0 Hz in F1 (^{1}HN), F2 (^{1}H), and F3 (^{15}N), respectively, with 512, 128, and 32 complex points. Carrier frequencies were 4.58 ppm for proton and 118 ppm for ^{15}N. Mixing times were between 65 and 100 ms for the NOESY experiments and 65 ms for the TOCSY. Three-dimensional sensitivity enhanced HNHB and HNHA experiments (*39*, *40*) were performed with carrier frequencies of 4.58 ppm in the proton dimensions and 114 ppm in the ^{15}N dimension and spectral widths of 5602.2, 2500.0, and 800.0 Hz in F1 (^{1}HN), F2 (^{1}H), and F3 (^{15}N), respectively, with 512, 72, and 28 complex points.

For paramagnetic line-broadening experiments, the protein concentration in each sample was ∼0.6 mM with the composition otherwise identical to that described above. ^{1}H,^{15}N HSQC experiments were recorded for each sample before and after addition of either 0.5 mM $MnCl_2$ or 2.5 mM 5- or 12-DOXYL-stearic acid. 1D ^{1}H spectra were also recorded to assess the effect of the paramagnetic agents on DPC resonances.

Data from all experiments was processed using NMRPipe (*41*) on LINUX workstations running REDHAT 6.0 or 7.3. A solvent filter was applied followed by processing using a 70°-shifted sine-bell squared window function. Data were zero filled prior to Fourier transformation and baseline correction. Linear prediction was applied in ^{15}N as appropriate. The software packages XEASY (*42*) and SPARKY (*43*) were used for spectral analysis.

Assignment of chemical shifts to the backbone amide groups of apoC-II was achieved using the ^{1}H,^{15}N NOESY−HSQC and ^{1}H,^{15}N TOCSY−HSQC spectra. Due to the α-helical nature of the protein, strong sequential NH−NH connectivities were observed in the ^{1}H,^{15}N NOESY−HSQC spectra, facilitating assignment by extended amide−amide walks. Assignment of aliphatic side-chain protons was achieved using the ^{1}H,^{15}N TOCSY−HSQC, HNHA, and HNHB, spectra, and sequential NOEs in the ^{1}H,^{15}N NOESY−HSQC spectra involving side-chain atoms were used to confirm the backbone assignments made on the basis of amide−amide connectivities. No attempt was made to assign the four prolines of apoC-II, side chain NH_2 groups, or aromatic protons. Secondary chemical shifts for αH and NH protons were calculated using the random coil chemical shift values of Wüthrich (*44*).

The software package DYANA (*45*) was used for the collation of structural constraints. NOE cross-peak intensities from the ^{1}H,^{15}N NOESY−HSQC spectrum was converted to upper limit distance constraints calibrated such that the

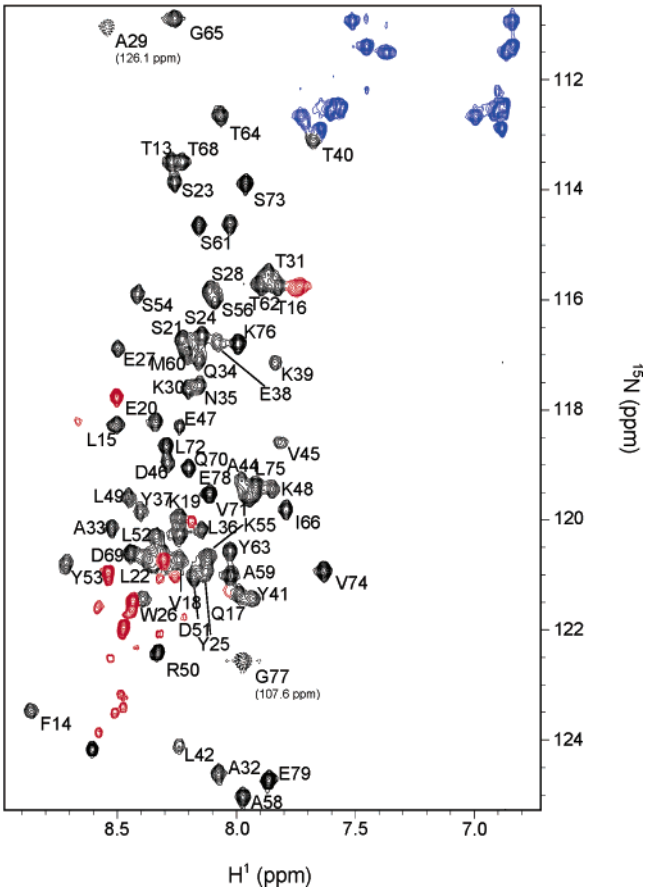

FIGURE 1: The ^{1}H,^{15}N HSQC spectrum of apoC-II in the presence of a 1:60 molar ratio of DPC in 20 mM sodium acetate, pH 5.0, at 30 °C. Asparagine and glutamine side chain NH_2 groups (blue) are identified as paired high-field ^{1}H with identical ^{15}N chemical shifts. Backbone amide resonances are labeled with their assigned residue. Unassigned residues are colored red. The resonances with dashed contour lines (A29 and G77) are "folded" in the ^{15}N dimension. Their true chemical shift is as labeled. The side chain indol resonance of W26 (at 10.64 ppm, 129.1 ppm) is omitted for clarity.

average sequential amide−amide distance constraint over the region of residues 26−35 was 2.8 Å. Only NOEs from 65 ms mixing time experiments were used in the calculation of distance constraints, and all NOEs that were ambiguous due to potential peak overlap or ambiguous side chain assignment were excluded from structure calculations.

The resulting unambiguous constraints served as input to structure calculations using torsion angle dynamics simulated annealing in CNS 0.9 (*46*). One hundred trial structures were calculated from extended chain starting conformers with different randomly assigned initial velocities. In the final Cartesian dynamics refinement step force constants of 50 kcal/(mol·Å^2) for NOE constraints and 200 kcal/(mol·rad^2) for dihedral angle constraints were used. A final family of structures was selected from the trial set by selecting those structures without NOE violations greater than 0.35 Å and with Lennard-Jones energies less than −25 kcal/mol.

RESULTS

Spectral Assignment and Collation of Structural Constraints. The ^{1}H,^{15}N HSQC spectrum of apoC-II in the presence of DPC micelles at 35 °C and pH 5 (Figure 1) is broadly similar to that observed in the presence of SDS under similar conditions (compare Figure 2 in ref *32*), though a number of significant differences are observable. There is a slight increase in dispersion in both the proton and ^{15}N dimensions in the DPC spectrum, while the line widths in DPC are slightly broader than those in SDS. Furthermore there is sufficient movement of individual peaks to require complete reassignment of the spectra acquired in DPC. In common with the ^{1}H,^{15}N HSQC acquired in SDS, the spectra in DPC shows a slight excess of backbone amide peaks above the 74 expected on the basis of the primary sequence of apoC-II as well as a small number of very weak peaks, consistent with some level of slow conformational exchange.

Spectral assignment of backbone amides, α-protons, and more than 80% of the observable nondegenerate aliphatic side-chain protons was achieved over residues 13−79. No attempt was made to assign the aromatics or side chain amides. Residues 1−12, which could not be assigned, are proline-rich and exhibit a paucity of interresidue NOEs. The assignment of Zdunek et al. (*33*) in SDS shows this region to be structurally ill-defined and the major source of the conformational heterogeneity inferred from the ^{1}H,^{15}N HSQC spectrum. It appears likely that this is also the case in DPC, as the unassigned ^{1}H,^{15}N HSQC cross-peaks are generally weak and the corresponding spin systems display only a few, weak inter- and intraresidue NOEs.

Sequential and medium-range NOEs were assigned from the ^{1}H,^{15}N NOESY−HSQC experiment based on the proton chemical shift assignments. These NOE data are presented in Figure 2, together with NOEs that cannot be unambiguously assigned due to peak overlap. The data are broadly similar to those determined from samples containing SDS with a strong general helical tendency shown by strong sequential HN−HN NOEs and many medium-range $i-i+3$ and $i-i+4$ NOEs throughout the sequence. Medium-range NOEs are particularly prevalent in large regions in the N-terminal half and C-terminal third of the molecule. The detailed distributions of these constraints do show some differences between the structure of apoC-II in DPC and that in SDS. In particular, the N-terminal helical region appears to be longer in DPC, as indicated by the longer stretch of medium-range NOEs in this region. In SDS, medium-range NOEs are particularly numerous through the residues 16−38, while in DPC this is extended to residues 14−41. There are also a number of medium-range NOEs across residues 42−52 in the DPC spectra, whereas there are very few such NOEs observed in the presence of SDS. A final difference between the DPC and SDS constraint data lies in the sequential HN−Hα NOEs, which are stronger and more numerous in the presence of DPC than in SDS, particularly in the region C-terminal of residue 52. NOEs of this type are typically strongest in extended backbone conformations and are usually weak in stable helical regions. Their presence here may indicate conformational exchange between a helical conformation and one more extended in nature, perhaps as a result of weaker interactions between apoC-II and the DPC micelle. Overall the number of NOEs unambiguously assignable is similar in each case.

As was the case with the SDS data (*32*, *33*), we were unable to unambiguously assign any long-range NOEs consistent with tertiary interactions. Their absence cannot be considered a conclusive indication of the absence of such interactions because interactions of this type are likely to be

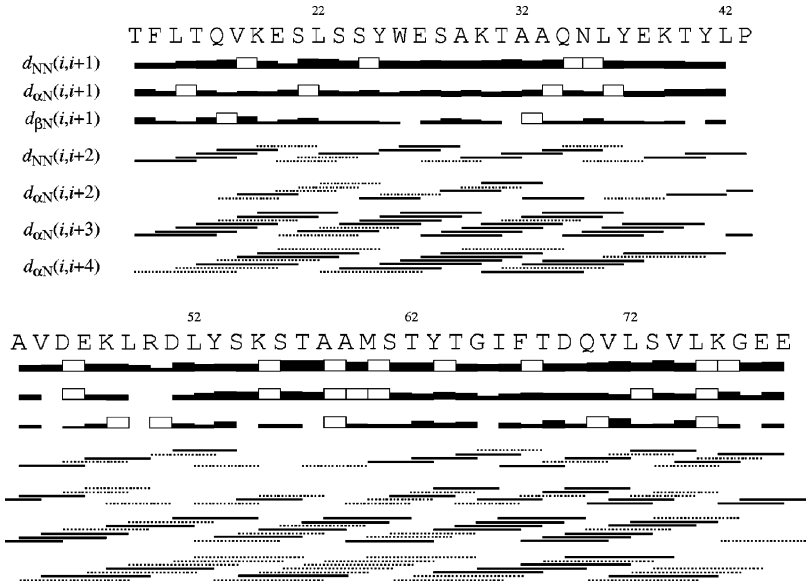

FIGURE 2: Summary of the sequential and medium-range constraints used in structural calculations. Unambiguously assigned sequential distance constraints are represented as solid bars with height indicative of the strength of the corresponding NOE with open bars indicating NOEs that are ambiguous due to resonance overlap and have not been included in structural calculations. Medium-range constraints are represented as solid lines with dotted lines indicating ambiguous constraints.

dominated by side chain−side chain contacts, which cannot be detected by the experiments performed here. Rather, the absence of this type of NOE means that no information is available from this study on the global conformation of apoC-II. On the other hand, the failure to detect any long-range NOEs in a total of three separate NMR investigations (the current study and refs *32* and *33*) suggests that there are unlikely to be significant tertiary interactions in the detergent-bound structure of apoC-II. In this respect, apoC-II appears to be similar to other apolipoproteins of similar size and function, such as apoC-I (*47*). Consistent with this idea, Zdunek et al. (*33*) find the helices of apoC-II to have distinct dynamic properties and to be orientated in an open U-shaped conformation lacking long-ranged protein−protein contacts but rather stabilized through interactions with the detergent micelle.

Secondary chemical shifts for Hα and HN residues have been calculated and are shown in Figure 3A. The patterns observed are strikingly similar to those seen in SDS (compare Figure 4A in ref *32*). Storjohann et al. also found a strong similarity between these two detergents when considering the chemical shifts of a C-terminal fragment of apoC-II (*48*). Storjohann et al. interpreted this similarity as indicating the functional equivalence of SDS and DPC as mimetics of the lipoprotein environment; however, poor spectral quality in DPC prevented a more detailed examination of this claim. The observation does, however, support the notion that the structure of apoC-II is not substantially different in the presence of DPC as compared to SDS. On the other hand, there are a number of potentially significant structural differences in apoC-II in these two detergents, which are detectable from further analysis of the NOE data, and these differences will be discussed in the following section.

The Fold of ApoC-II. CNS calculations using constraints derived from measured NOE connectivities as summarized in Figures 2 and 3 and Table 1 were used to determine detailed structures of apoC-II. Of 100 calculated structures, 18 were selected for further analysis on the basis of distance

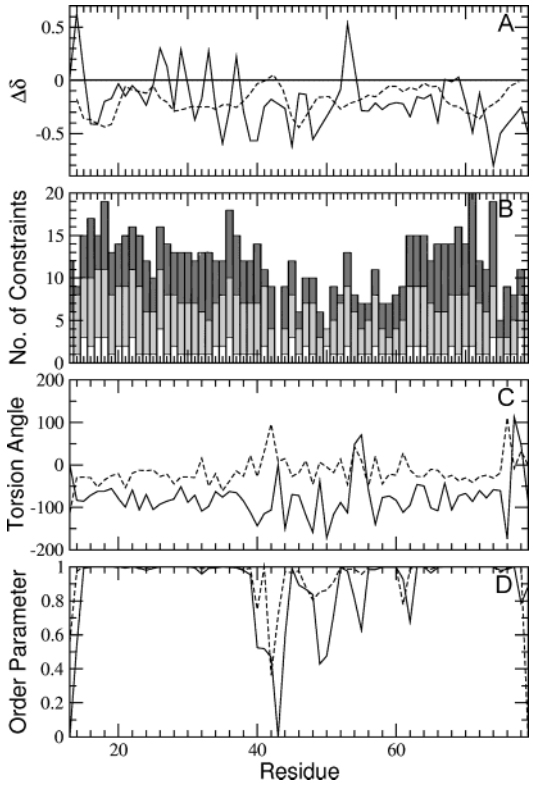

FIGURE 3: Panel A shows secondary chemical shifts for Hα (− − −) and HN (—) of each residue. Hα shifts are presented as a three-point running average. In panel B, the number of distance constraints per residue is presented with white bars representing intraresidue constraints, pale gray bars representing sequential constraints, and dark gray bars representing medium-range ($i - j < 5$) constraints. The average angle (C) and associated order parameters (D) of the backbone torsion angles ϕ (—) and ψ (− − −) for each residue over the family of 18 calculated structures are also presented.

constraint violations and Lennard-Jones energies. A summary of the structural statistics for this family of structures is presented in Table 1. The backbone torsion angles (ϕ and ψ) for the calculated structures are presented in Figure 3C

Table 1: Statistics for the Accepted Structures of ApoC-II

No. of Unambiguous NOE-Derived Distance Constraints	
total	444
intraresidue ($i = j$)	101
sequential ($i - j = 1$)	181
medium-range ($i - j < 5$)	162

Constraint Violations

	average[a]	best[b]
no. of distance violations >0.2 Å	0.3 ± 0.5	0
largest distance violation (Å)	0.19 ± 0.09	0.12
RMSD from distance constraints (Å)	0.026 ± 0.004	0.021

Structural Energies (kcal/mol)

total	28 ± 14	5.4
bond	2.8 ± 0.7	1.9
angle	36 ± 2	33
Lennard-Jones	−36 ± 9	−52
distance constraint	23 ± 7	15

Backbone Atom RMSDs (Å)[c]

residues 14−39	1.3
residues 14−24	0.17
residues 24−32	0.18
residues 32−39	0.19
residues 64−78	0.29

[a] Average values ± standard deviation calculated for the 18 accepted structures. [b] Best values for the 18 accepted structures. [c] Average pairwise RMSDs of atomic coordinates of C, Cα, and N for indicated residues across 18 accepted structures.

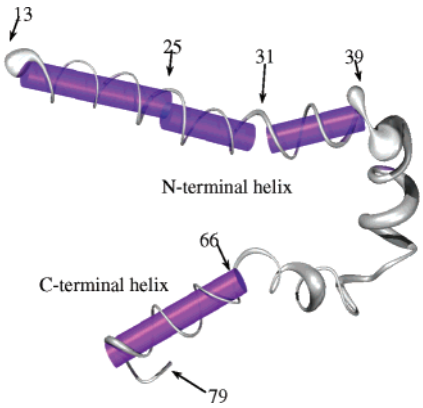

FIGURE 4: A representative calculated structure of apoC-II, presented as an α-carbon trace with line width drawn to represent angular variance of the ϕ torsion angle over the family of 18 calculated structures. Narrow line width indicates well-defined structure, while broader line width indicates more poorly defined structure. The helical axes of regions of well-defined helicity are indicated with cylinders. The N- and C-terminal helical regions are labeled, as is the position of significant residues (see text for details).

with the associated order parameters in Figure 3D. These torsion angles are consistent with helical structure over most of the sequence, and order parameters close to unity (indicating well-defined local structure) are observed for residues 15−39 and 63−77.

A representative backbone conformation selected from the calculated structures is shown in Figure 4. In the N-terminal half of the molecule is an extended helix over residues 13−39 interrupted by small kinks in the helix at residue 24 and residue 32. This region is believed to be the major lipid-binding domain of apoC-II, and as noted previously, this region is amphipathic with the characteristic charge distribution of a class A_2 amphipathic helix. Helical structure is seen across the family of accepted structures, though the overall precision for this region is low with an average pairwise RMSD for the backbone heavy atom coordinates of 1.4 Å across these residues. Closer examination reveals that the lack of precision is centered on the two distortions of ideal helical conformation at residues 24 and 32. Figure 3D shows that the torsion angle order parameters for these residues are slightly reduced and the backbone atomic RMSDs for the intervening regions (14−24, 24−32, 32−39) are all below 0.2 Å (Table 1). Resonance overlap obscures a number of medium-range NOEs near to residues 24 and 32, and it is likely that the consequent lack of unambiguous distance constraint data is the cause of the apparent lack of order at these residues.

As observed from the torsion angle order parameters, the C-terminal half of apoC-II is comparatively less ordered than the N-terminal helix, although a clear helical tendency is seen throughout most of the region. The most ordered helical region of the C-terminal half of the molecule spans residues 63−77, and this helix is capped at the extreme C terminus by an unusual turn-like structure also seen in the SDS structure (*32*) and in other work (*48*, *49*). In this structure, G77 bends back, redirecting the peptide backbone in the opposite direction to the helical twist of the preceding residues and projecting E78 and E79 back along the hydrophilic face of the helix (Figure 4). The central region, comprising residues 40−65, is substantially disordered despite having a significant role in the activation of LpL. Fewer NOEs are assignable within this region than can be assigned over the rest of the molecule. Examination of Figure 2 does reveal a number of ambiguous NOEs over this region, owing to chemical shift degeneracy impeding NOE assignment. Because of this it is not possible to determine whether the observed disorder reflects genuine structural heterogeneity or whether it merely reflects the lack of unambiguous data.

Separating the N- and C-terminal halves of the apoC-II molecule is a short, highly unstructured region centered on P43. Both in the current data and in the data acquired in SDS, this region lacks medium-range NOEs. On this basis and on the basis of the relaxation measurements of Zdunek et al. (*33*), it appears that this region might form a flexible nonhelical hinge that separates the functionally distinct halves of the apoC-II molecule, allowing them to adopt a loosely antiparallel arrangement on the detergent micelle.

ApoC-II/Detergent Interactions. Intermolecular NOEs between apoC-II backbone amides and the protons of the DPC aliphatic chain were identified in the ^{1}H,^{15}N NOESY−HSQC spectrum, and these NOEs are summarized in Figure 5A. All NOEs detected are to the broad resonance at 1.32 ppm, corresponding to methylene groups 3−11 of DPC or to the resonance at 1.63 ppm corresponding to methylene 2 of DPC (see Figure 6). Interactions with the detergent molecule appear in general to display the 3−4 residue periodicity expected for a helix lying parallel to the surface of a detergent micelle. In particular such periodic contacts are seen over residues 19−29, 45−52, and 56−63. Additional contacts, which show no obvious periodicity, are seen in the regions 36−42 and 73−77. It is interesting to note that the regions 45−52 and 56−63 do not correspond to helical regions that are well defined by the distance constraint data; the observation of periodic detergent contacts in this region, together with the other suggestions of helical conformation such as the sequential HN−HN NOEs (Figure

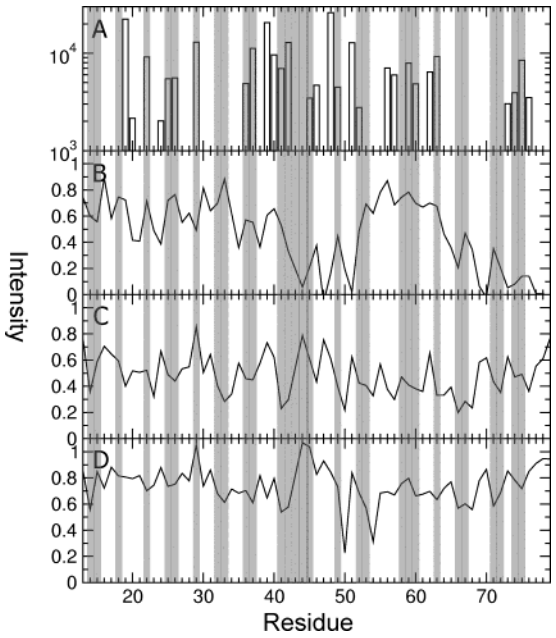

FIGURE 5: NOE intensities (A) between backbone NH resonances of apoC-II and the acyl methylene groups of DPC and (B,C,D) broadening of apoC-II backbone NH resonances by paramagnetic agents. Peak height for each resonance in the presence of DPC and Mn^{2+} (B), 5-DOXYL-stearic acid (C), and 12-DOXYL-stearic acid (D) are expressed as a fraction of the peak height in the presence of DPC alone. Positions corresponding to hydrophobic or aromatic residues in apoC-II are shaded.

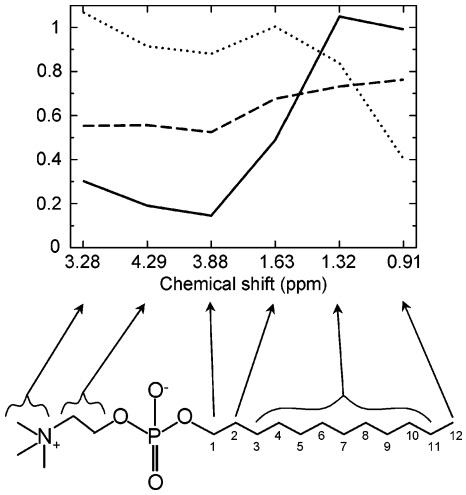

FIGURE 6: Broadening of DPC ^1H resonances by paramagnetic agents. Peak height for each resonance in the presence of 0.5 mM Mn^{2+} (—), 2.5 mM 5-DOXYL-stearic acid (− − −), and 2.5 mM 12-DOXYL-stearic acid (•••) are expressed as a fraction of the peak height in the absence of paramagnetic agent. The resonances of protons on carbons 3−11 of the aliphatic chain are not clearly resolved in the 1D NMR spectra.

2) and the average torsion angle values (Figure 3C), suggests that despite the lack of unambiguous distance constraint data, these regions do adopt a helical conformation in the presence of DPC.

Of particular note are the interactions between the protons on carbon 2 of the DPC aliphatic chain and the backbone amide of K19, K39, and K48. These three lysine residues are all in regions with the potential to form class A_2 α-helices, although the helix around residue 48 appears only weakly ordered by the structural data described here. According to the snorkel hypothesis for the interaction of apolipoproteins with the lipoprotein surface, lysine residues within class A_2 amphipathic helices are predicted to "snorkel" out of the lipid monlayer such that their positively charged primary amine can interact with the lipid phosphate moiety. In such a conformation, the backbone of the lysine residues will be exposed to contacts with the lipid fatty acid chains. If a similar conformation were adopted in the interaction of apoC-II with DPC, then NOEs such as are observed for K19, K39, and K48 would be expected. Thus, these NOEs demonstrate that DPC molecules are interacting with these lysine residues in a manner similar to that predicted by the snorkel hypothesis.

To gain a more detailed picture of the interactions between apoC-II and DPC, we have collected ^1H,^{15}N HSQC spectra in the presence of paramagnetic agents expected to partition within particular regions of the micellar DPC sample. Initially one-dimensional ^1H NMR spectra of DPC were recorded in the presence of each of the paramagnetic agents. Each agent selectively broadened signals from the expected part of the DPC molecule (Figure 6), confirming that each paramagnetic species broadened NMR signals in a spatially selective fashion: Mn^{2+} broadened only those signals originating from protons of the phosphocholine headgroup, while 12-DOXYL-stearic acid affected only protons close to the core of the micelle. 5-DOXYL-strearic acid broadened resonances throughout the DPC molecule in an approximately equal fashion. On the basis of these findings, we can conclude that backbone amide resonances of apoC-II that are preferentially broadened by Mn^{2+} are preferentially solvent-exposed under our experimental conditions, whereas those preferentially broadened by 5-DOXYL-stearic acid or 12-DOXYL-stearic acid are exposed to the DPC micelle. The degree of line-broadening induced by each paramagnetic agent was quantified by comparing the peak height of each resonance in the presence of the agent to that measured from the same sample prior to the addition of the agent. The results of these experiments are presented in Figure 5B−D.

Mn^{2+} causes a significant reduction in peak height for all resonances of apoC-II, indicating that the entire protein is to some degree exposed to the aqueous environment. This is consistent with a reversible protein/detergent interaction similar to the reversible interaction of apoC-II with the lipoprotein surface. A local 3−4 residue periodicity can be detected throughout much of the molecule that corresponds with the periodicity observed for the intermolecular NOEs (Figure 5A). Many of the residues involved in intermolecular NOEs show greater protection from Mn^{2+} than do nearby residues that do not show NOEs to DPC. Furthermore the observed periodicity of Mn^{2+} exposure follows closely the pattern of hydrophobicity in the apoC-II sequence with most peaks in Figure 5B (indicating protection from Mn^{2+}) corresponding to hydrophobic residues. This provides further evidence that apoC-II interacts with DPC as a series of amphipathic α-helices lying flat on the micelle surface. In addition, two regions of apoC-II, residues 42−52 and 64−79, show significantly greater solvent exposure than the rest of the molecule, as indicated by their reduced normalized peak height relative to other residues. Interestingly both intermolecular NOEs to the DPC aliphatic chain and periodic variations in Mn^{2+} exposure are seen even in the regions showing highest overall solution exposure. This suggests that these regions do interact with the DPC micelle in helical

form, albeit with reduced affinity as compared to the other regions of apoC-II.

The effects of the two DOXYL-stearic acids support this view of the apoC-II/DPC interaction: in both cases, a 3−4 residue periodicity is seen in the normalized peak heights that is out of phase with the periodicity observed in the presence of Mn^{2+}, consistent with the suggestion that this periodicity arises from the differential solvent and detergent accessibility of a helix lying on the micelle surface. Furthermore the central and C-terminal regions of apoC-II, which are highly solvent-exposed, show slightly reduced exposure to the paramagnetic groups of the DOXYL-stearic acid derivatives. In general, the levels of broadening seen are greater for 5-DOXYL-strearic acid than they are for 12-DOXYL-stearic acid, adding further support to the hypothesis of an interaction at the surface of the micelle.

DISCUSSION

The structure of apoC-II has previously been determined by us (*32*) and by others (*33*) in the presence of SDS. Although SDS has proved to be a reasonable mimic of lipid surfaces for many structural studies of apolipoproteins and other lipid-associating proteins, there remain a number of ongoing concerns regarding its use. In particular, it is difficult to interpret structural data pertaining to protein/detergent interactions in terms of native protein/lipid interactions due to the chemical dissimilarity between SDS and biologically relevant lipid species. As demonstrated by the results presented here, the use of DPC, which is similar in headgroup and chain length to phosphatidyl choline, provides a valuable alternative to SDS in this respect.

The structure of apoC-II determined in DPC is broadly similar to that in SDS, suggesting that the specific chemical nature of the water/lipid interface provided by phospholipid is not necessary for the correct structural interactions of apolipoproteins with lipoprotein particles. Rather the data suggests that any amphipathic interface will suffice. Despite this broad similarity, a number of differences between the two structures are evident on closer examination. In particular, the ordered N-terminal lipid-binding helix is extended at both its N- and its C-terminal ends, such that in DPC it spans residues 13−39 whereas in SDS it is limited to residues 17−36. The more extensive lipid-binding helix in the presence of DPC might be taken as evidence that a different mode of detergent interactions acts to stabilize the helix in DPC than is the case in SDS. Contrasting with the N-terminus, the C-terminal half of the protein shows a general reduction in ordered helical content with respect to the structure in SDS. Most notably, a disruption of helical structure around residue 63 is seen in DPC that was absent in SDS. This disruption has been suggested elsewhere to be important for LpL activation because Y63 is known to be a critical residue in this process and the break in helical conformation was proposed to project this residue away from the lipoprotein surface to enable interaction with LpL (*48*). Due to the possibility that the conformational disorder observed here reflects a lack of assignable NOEs rather than true structural instability and in the absence of structural data in the presence of LpL, we are not able to offer evidence in support of this claim.

One of the most notable structural features of the lipid binding helix as determined in SDS was a bend that makes the hydrophobic face of the helix convex. We have hypothesized that it might have a role in the specificity of lipid interactions in vivo and were thus interested to confirm its presence in DPC. The NOEs from S23 and S24 to E27 which were shown to be critical in defining this feature in SDS are also present in the spectrum acquired in DPC at approximately equivalent intensity. However the ambiguity of a number of other medium-range NOEs in this region, most notably due to the chemical shift degeneracy of the Hα of residues 22 and 24, means that the data acquired in DPC is insufficient to constrain the direction of the bend and both convex and concave helical conformations are seen. As a result we are unable to confirm the presence of the unusual helical bend seen in SDS. Several other medium-range NOEs in this area are also ambiguous in the DPC data (Figure 3), and it therefore seems likely that the disorder seen here is due to a lack of sufficient data in the region. For this reason, no significance can be attached to our failure to detect the helical bend in the DPC structure, and this region remains an interesting area for future study of the basis for the preferential interactions of apoC-II with larger triacylglycerol-rich lipoprotein particles.

The nature of the interaction between apolipoproteins and the lipoprotein surface remains poorly understood at all but the most basic of levels. In particular, although it is well-known that apolipoproteins interact with lipid surfaces via amphipathic helices with specific charge distributions, the structural determinants of the interaction are not clear. Here we define in detail the interaction of apoC-II with the DPC micelle. The emergent picture of the interactions between apoC-II and DPC is that the majority of the protein forms amphipathic helices, which interact reversibly with the surface of the detergent micelle in a manner similar to the proposed interactions between apoC-II and the phospholipid surface of the lipoprotein particle. Despite the fact that most of apoC-II shows clear evidence of close contact with the micellar surface, the protein also shows significant solvent exposure as evidenced by its susceptibility to line-broadening by Mn^{2+}. This solvent exposure is not uniform, and two regions comprising residues 42−52 and 64−79 show greater solvent exposure, suggesting reduced affinity for the detergent micelle. Both of these regions are amphipathic, so it is of some interest to consider possible reasons for this reduced affinity for the detergent surface. In the case of residues 42−52, P43 presents itself as a potential culprit: proline residues are well-known to disrupt helical structure and on the basis of the available structural evidence, P43 appears to do so here. As described previously (*32*), the helical region around residues 59−76 shows a significant distortion from an ideal amphipathic arrangement with two hydrophobic clusters that are 120° out of alignment about the helical axis. Furthermore, the structure of this region, particularly around residue 63, shows significant disorder and some deviation from an ideal α-helical conformation in the presence of DPC. It seems likely that the reduced affinity of the C-terminal helix arises as a result of the distortion to amphipathicity and that some degree of flexibility centered near residue 63 permits the extreme C-terminal region to exchange on and off the micelle surface. Indeed, Zdunek et al. (*33*) found that the helical region 65−75 displayed elevated levels of motion on the nanosecond time scale, as compared to the other helical regions in their structure in SDS. This motion is accounted

for as a domain-like rigid motion of this C-terminal helix and so is supportive of the idea that in both detergent environments this region exchanges on and off the micelle surface.

Intermolecular NOEs between apoC-II and DPC indicate that the structure of the protein/detergent complex is similar to that proposed by the snorkel hypothesis. Specifically, these NOEs show a strong periodicity over much of the protein, consistent with the amphipathic helices lying flat at the surface of the detergent micelle. In addition, specific contacts are seen between three lysine residues of apoC-II and the DPC aliphatic chain near the phosphate of the headgroup, consistent with the snorkel-like orientation of lysine residues from which the snorkel hypothesis gets its name. However, the similarity between the apoC-II structures determined in SDS and DPC suggests that these DPC-specific contacts are not the primary factors driving the affinity of apoC-II for detergent surfaces.

It is of some interest, therefore, to compare the NOEs detected between apoC-II and SDS to those detected to DPC (Figure 7 in ref *32*). Such comparison reveals a lack of discernible periodicity in the SDS contacts. It is possible that spin diffusion obscures the details of the protein/detergent interaction; however, it is not clear why this should be the case for SDS but not for DPC. Alternatively the lack of periodicity in the SDS contacts might reflect structural differences between the two protein/detergent complexes. In particular, it might be that the helices of apoC-II bind at the surface of the SDS micelle, but the surface is dynamically disordered to such an extent as to obscure the expected periodicity in the protein/detergent complexes. It might also be the case that apoC-II is in fact buried in the center of the SDS micelle with its helices exposed at all sides to the aliphatic chains of the detergent. Either of these conclusions have implications for the work of ref *33*, which has modeled the structure of the apoC-II/SDS complex based on NMR relaxation data and assuming the SDS micelle to be a static, spherical structure with apoC-II at its surface.

It appears likely, on the basis of these observations, that the snorkel hypothesis accurately describes the structure of the complex between apoC-II and the lipoprotein surface but that the specific contacts between the protein and the lipid headgroup implied by the snorkel hypothesis are not necessary for this interaction. Instead, nonspecific interactions between the amphipathic helix and the amphipathic surface dominate. On this basis, we might predict the apoC-II/SDS complex to be less structurally defined because it is based solely on these nonspecific interactions, whereas the complex with DPC has specific protein/headgroup interactions adding definition to the structure of the complex. Such factors might account for the observed differences between the two detergents at two levels: the different patterns of intermolecular NOEs and the extension to the N-terminal lipid-binding helix seen in DPC.

Despite extensive study, the mechanism of activation of LpL by apoC-II remains obscure, as does the structural basis for the interaction between the two proteins. It is known that the C-terminal half of apoC-II is responsible and some evidence suggests an apoC-II binding site near the active site of LpL. Given this, it is of interest to consider aspects of the apoC-II C-terminal structure that might be consistent with such an interaction. The most obvious and unusual feature of the C-terminal half of apoC-II is the turn-like structure that caps the helix at the extreme C-terminus. This feature has been observed previously to have unusual stability considering its position, prompting the suggestion that it is likely to be of functional importance. A number of biochemical studies have implicated the extreme C-terminus of apoC-II as a binding site for LpL, and the tetrapeptide KGEE corresponding to this region acts as a competitive inhibitor of LpL activation by apoC-II, implying that the C-terminus is important for binding to LpL but not directly responsible for activation (*50*). On the basis of homology modeling against pancreatic lipase, a number of putative basic patches on the surface of LpL have been identified. Several of these patches have also been implicated in the apoC-II/LpL interaction, raising the possibility that the negative charges at the C-terminus of apoC-II engage in salt bridges with these basic surfaces on LpL thereby tethering apoC-II to the enzyme (*51*, *52*). It is proposed that once so tethered, apoC-II could offer other lower-affinity regions to engage in the activating interactions.

Sequences of apoC-II from 10 animal species are available, and across these sequences nine residues are absolutely conserved (*53*). Of these, seven residues are found in the region 59−70, arranged such that if this region were helical, all seven would fall on the same side of the helix, at the interface between the hydrophobic and hydrophilic faces (*54*). It is therefore tempting to postulate that residues 59−70 might comprise a helical LpL binding domain on apoC-II. The helical structure of this region is not, however, clear from the available data. In the data acquired in SDS the region is helical, although residues 59−63 are considerably less ordered than are those toward the C-terminus (*32*, *33*). In DPC, the apparent disorder is even greater with all residues N-terminal of I66 showing significant disorder based on the available distance constraints. Furthermore, the analysis of paramagnetic line-broadening presented here suggests that residues 64−79 show reduced affinity for the DPC micellar surface as demonstrated by increased exposure to Mn^{2+} and reduced exposure to paramagnetic probes partitioned within the micelle. It is not clear whether this observation is specific to the detergent system or whether such differential affinity would also apply to the apoC-II/lipoprotein interaction. However, it is consistent with the increased degree of nanosecond motion detected in this region in SDS (*33*). It is attractive, then, to hypothesize that the C-terminal helix, residues 66−79, might, by virtue of a region of flexibility near Y63, be capable of disengaging from the lipoprotein surface to bind LpL.

There is also evidence to suggest that other regions nearer the center of the apoC-II sequence might also be involved in the LpL interaction (*5*). The residues in this central region that might be involved in the apoC-II/LpL interaction remain very poorly defined, however. Some hints at the structural basis for these interactions are available from recent results. A circular dichroism study of the complex of apoC-II_{39-62} and LpL indicates a substantial increase in α-helical structure in the complex, as compared to the two components in isolation (*55*). Because apoC-II_{39-62} is unstructured in the absence of LpL but is predicted to form an amphipathic α-helix, it is likely that helical conformation is induced in the peptide on binding to LpL. However the magnitude of the observed change in the CD spectrum is indicative of

approximately 30 residues changing from an unstructured to a helical conformation, suggesting that some part of LpL must also undergo such a conformational transition. It is significant to note that the colipase-mediated interfacial activation of pancreatic lipase is associated with an increase in helical structure in the 24 residue loop, which acts as a lid over the active site. Perhaps, then, the central region of apoC-II interacts with LpL in such a way as to stabilize the open, active conformation of the LpL lid with this interaction also stabilizing the helical conformation of apoC-II in this region. A possible mode for such an interaction is suggested by computational docking of the C-terminal third of apoC-II to LpL, which reveals a possible binding site for a helical stretch of apoC-II in the cleft between the N- and C-terminal domains of LpL such that contacts are also made to the open conformation of the LpL loop (*56*).

SUPPORTING INFORMATION AVAILABLE

A table of chemical shifts of assigned resonances in apoC-II and a figure showing the ^{15}N-TOCSY−HSQC and the HNHB spectra of residues 13−21. This material is available free of charge via the Internet at http://pubs.acs.org.

REFERENCES

1. Fojo, S. S., Law, S. W., and Brewer, H. B., Jr. (1984) Human apolipoprotein C-II: complete nucleic acid sequence of preapolipoprotein C-II, *Proc. Natl. Acad. Sci. U.S.A. 81*, 6354−6357.
2. Havel, R. J., Fielding, C. J., Olivecrona, T., Shore, V. G., Fielding, P. E., and Egelrud, T. (1973) Cofactor activity of protein components of human very low-density lipoproteins in the hydrolysis of triglycerides by lipoproteins lipase from different sources, *Biochemistry 12*, 1828−1833.
3. Eckel, R. H. (1989) Lipoprotein lipase. A multifunctional enzyme relevant to common metabolic diseases, *N. Engl. J. Med. 320*, 1060−1068.
4. Clarke, A. R., and Holbrook, J. J. (1985) The mechanism of activation of lipoprotein lipase by apolipoprotein C-II. The formation of a protein−protein complex in free solution and at a triacylglycerol/water interface, *Biochim. Biophys. Acta 827*, 358−368.
5. MacPhee, C. E., Hatters, D. M., Sawyer, W. H., and Howlett, G. J. (2000) Apolipoprotein C-II39−62 activates lipoprotein lipase by direct lipid-independent binding, *Biochemistry 39*, 3433−3440.
6. Segrest, J. P., Jones, M. K., De Loof, H., Brouillette, C. G., Venkatachalapathi, Y. V., and Anantharamaiah, G. M. (1992) The amphipathic helix in the exchangeable apolipoproteins: a review of secondary structure and function, *J. Lipid Res. 33*, 141−166.
7. Segrest, J. P., De Loof, H., Dohlman, J. G., Brouillette, C. G., and Anantharamaiah, G. M. (1990) Amphipathic helix motif: classes and properties, *Proteins 8*, 103−117.
8. Segrest, J. P., Jackson, R. L., Morrisett, J. D., and Gotto, A. M., Jr. (1974) A molecular theory of lipid−protein interactions in the plasma lipoproteins, *FEBS Lett. 38*, 247−258.
9. Kanellis, P., Romans, A. Y., Johnson, B. J., Kercret, H., Chiovetti, R., Jr., Allen, T. M., and Segrest, J. P. (1980) Studies of synthetic peptide analogues of the amphipathic helix. Effect of charged amino acid residue topography on lipid affinity, *J. Biol. Chem. 255*, 11464−11472.
10. Anantharamaiah, G. M., Jones, J. L., Brouillette, C. G., Schmidt, C. F., Chung, B. H., Hughes, T. A., Bhown, A. S., and Segrest, J. P. (1985) Studies of synthetic peptide analogues of the amphipathic helix. Structure of complexes with dimyristoyl phosphatidylcholine, *J. Biol. Chem. 260*, 10248−10255.
11. Fukushima, D., Yokoyama, S., Kroon, D. J., Kezdy, F. J., and Kaiser, E. T. (1980) Chain length-function correlation of amphiphilic peptides. Synthesis and surface properties of a tetratetracontapeptide segment of apolipoprotein A−I, *J. Biol. Chem. 255*, 10651−10657.
12. Sparrow, J. T., Ferenz, C. R., Gotto, A. M., Jr., and Pownall, H. J. (1981) in *Peptides: Synthesis-Structure-Function* (Roch, D., and Gross, E., Eds.) pp 253−256, Pierce Chemical Company, Rockford, IL.
13. Mao, S. J., Sparrow, J. T., Gilliam, E. B., Gotto, A. M., Jr., and Jackson, R. L. (1977) Mechanism of lipid−protein interaction in the plasma lipoproteins: lipid-binding properties of synthetic fragments of apolipoprotein A-II, *Biochemistry 16*, 4150−4156.
14. Chen, T. C., Sparrow, J. T., Gotto, A. M., Jr., and Morrisett, J. D. (1979) Apolipoprotein A-II: chemical synthesis and biophysical properties of three peptides corresponding to fragments in the amino-terminal half, *Biochemistry 18*, 1617−1622.
15. Jackson, R. L., Morrisett, J. D., Sparrow, J. T., Segrest, J. P., Pownall, H. J., Smith, L. C., Hoff, H. F., and Gotto, A. M., Jr. (1974) The interaction of apolipoprotein-serine with phosphatidylcholine, *J. Biol. Chem. 249*, 5314−5320.
16. Catapano, A. L., Kinnunen, P. K., Breckenridge, W. C., Gotto, A. M., Jr., Jackson, R. L., Little, J. A., Smith, L. C., and Sparrow, J. T. (1979) Lipolysis of ApoC-II deficient very low-density lipoproteins: enhancement of lipoprotein lipase action by synthetic fragments of apoC-II, *Biochem. Biophys. Res. Commun. 89*, 951−957.
17. Sparrow, J. T., Gotto, A. M., Jr., and Morrisett, J. D. (1973) Chemical synthesis and biochemical properties of peptide fragments of apolipoprotein-alanine, *Proc. Natl. Acad. Sci. U.S.A. 70*, 2124−2128.
18. Sparrow, J. T., Pownall, H. J., Hsu, F. J., Blumenthal, L. D., Culwell, A. R., and Gotto, A. M. (1977) Lipid binding by fragments of apolipoprotein C-III-1 obtained by thrombin cleavage, *Biochemistry 16*, 5427−5431.
19. Srinivas, R. V., Venkatachalapathi, Y. V., Rui, Z., Owens, R. J., Gupta, K. B., Srinivas, S. K., Anantharamaiah, G. M., Segrest, J. P., and Compans, R. W. (1991) Inhibition of virus-induced cell fusion by apolipoprotein A−I and its amphipathic peptide analogues, *J. Cell. Biochem. 45*, 224−237.
20. Sparrow, J. T., and Gotto, A. M., Jr. (1982) Apolipoprotein/lipid interactions: studies with synthetic polypeptides, *CRC Crit. Rev. Biochem. 13*, 87−107.
21. Sparrow, J. T., Sparrow, D. A., Fernando, G., Culwell, A. R., Kovar, M., and Gotto, A. M., Jr. (1992) Apolipoprotein E: phospholipid binding studies with synthetic peptides from the carboxyl terminus, *Biochemistry 31*, 1065−1068.
22. Lux, S. E., Hirz, R., Shrager, R. I., and Gotto, A. M. (1972) The influence of lipid on the conformation of human plasma high-density apolipoproteins, *J. Biol. Chem. 247*, 2598−2606.
23. Pownall, H. J., Hsu, F. J., Rosseneu, M., Peeters, H., Gotto, A. M., and Jackson, R. L. (1977) Thermodynamics of lipid protein associations. Thermodynamics of helix formation in the association of high-density apolipoprotein A-I (apoA-I) to dimyristoyl phosphatidylcholine, *Biochim. Biophys. Acta 488*, 190−197.
24. Massey, J. B., Gotto, A. M., Jr., and Pownall, H. J. (1979) Contribution of alpha helix formation in human plasma apolipoproteins to their enthalpy of association with phospholipids, *J. Biol. Chem. 254*, 9559−9561.
25. Chung, B. H., Anatharamaiah, G. M., Brouillette, C. G., Nishida, T., and Segrest, J. P. (1985) Studies of synthetic peptide analogs of the amphipathic helix. Correlation of structure with function, *J. Biol. Chem. 260*, 10256−10262.
26. Lund-Katz, S., Phillips, M. C., Mishra, V. K., Segrest, J. P., and Anantharamaiah, G. M. (1995) Microenvironments of basic amino acids in amphipathic alpha-helices bound to phospholipid: 13C NMR studies using selectively labeled peptides, *Biochemistry 34*, 9219−9226.
27. Mishra, V. K., Palgunachari, M. N., Segrest, J. P., and Anantharamaiah, G. M. (1994) Interactions of synthetic peptide analogs of the class A amphipathic helix with lipids. Evidence for the snorkel hypothesis, *J. Biol. Chem. 269*, 7185−7191.
28. Epand, R. M., Surewicz, W. K., Hughes, D. W., Mantsch, H., Segrest, J. P., Allen, T. M., and Anantharamaiah, G. M. (1989) Properties of lipid complexes with amphipathic helix-forming peptides. Role of distribution of peptide charges, *J. Biol. Chem. 264*, 4628−4635.
29. Mehta, R., Gantz, D. L., and Gursky, O. (2003) Effects of mutations in apolipoprotein C-1 on the reconstitution and kinetic stability of discoidal lipoproteins, *Biochemistry 42*, 4751−4758.
30. Mehta, R., Gantz, D. L., and Gursky, O. (2003) Human plasma high-density lipoproteins are stabilized by kinetic factors, *J. Mol. Biol. 328*, 183−192.
31. Gursky, O., Ranjana, and Gantz, D. L. (2002) Complex of human apolipoprotein C-1 with phospholipid: thermodynamic or kinetic stability? *Biochemistry 41*, 7373−7384.

32. MacRaild, C. A., Hatters, D. M., Howlett, G. J., and Gooley, P. R. (2001) NMR structure of human apolipoprotein C-II in the presence of sodium dodecyl sulfate, *Biochemistry 40*, 5414−5421.
33. Zdunek, J., Martinez, G. V., Schleucher, J., Lycksell, P. O., Yin, Y., Nilsson, S., Shen, Y., Olivecrona, G., and Wijmenga, S. (2003) Global structure and dynamics of human apolipoprotein CII in complex with micelles: evidence for increased mobility of the helix involved in the activation of lipoprotein lipase, *Biochemistry 42*, 1872−1889.
34. Hatters, D. M., MacPhee, C. E., Lawrence, L. J., Sawyer, W. H., and Howlett, G. J. (2000) Human apolipoprotein C-II forms twisted amyloid ribbons and closed loops, *Biochemistry 39*, 8276−8283.
35. Bodenhausen, D., and Ruben, D. J. (1980) Natural abundance nitrogen-15 NMR by enhanced heteronuclear spectroscopy, *Chem. Phys. Lett. 69*, 185−189.
36. Fesik, S. W., and Zuiderweg, E. R. P. (1988) Heteronuclear 3-dimensional NMR-spectroscopy − A strategy for the simplification of homonuclear two-dimensional NMR-specra, *J. Magn. Reson. 78*, 588−593.
37. Marion, D., Kay, L. E., Sparks, S. W., Torchia, D. A., and Bax, A. (1989) Three-dimensional heteronuclear NMR of nitrogen-15 labeled proteins, *J. Am. Chem. Soc. 111*, 1515−1517.
38. Vuister, G. W., and Bax, A. (1993) Quantitative J correlation: a new approach for measuring homonuclear three-bond J(HNHα) coupling constants in 15N-enriched proteins, *J. Am. Chem. Soc. 115*, 7772−7777.
39. Archer, S. J., Ikura, M., Torchina, D. A., and Bax, A. (1991) An alternative 3D-NMR technique for correlating backbone ^{15}N with side chain Hβ-resonances in larger protiens, *J. Magn. Reson. 95*, 636−641.
40. Zhang, O., Kay, L. E., Olivier, J. P., and Forman-Kay, J. D. (1994) Backbone ^{1}H and ^{15}N resonance assignments of the N-terminal SH3 domain of drk in folded and unfolded states using enhanced-sensitivity pulsed field gradient NMR techniques, *J. Biomol. NMR 4*, 845−858.
41. Delaglio, F., Grzesiek, S., Vuister, G. W., Zhu, G., Pfeifer, J., and Bax, A. (1995) NMRPipe: a multidimensional spectral processing system based on UNIX pipes, *J. Biolmol. NMR 6*, 277−293.
42. Bartels, C., Xia, T. H., Billeter, M., Guntert, P., and Wüthrich, K. (1995) The program XEASY for computer-supported NMR spectral analysis of biological macromolecules, *J. Biolmol. NMR 6*, 1−10.
43. Goddard, T. D., and Kneller, D. G. (2002) *SPARKY*, University of California, San Francisco, San Francisco.
44. Wüthrich, K. (1986) *NMR of Proteins and Nucleic Acids*, Wiley, New York.
45. Guntert, P., Mumenthaler, C., and Wuthrich, K. (1997) Torsion angle dynamics for NMR structure calculation with the new program DYANA, *J. Mol. Biol. 273*, 283−298.
46. Brunger, A. T., Adams, P. D., Clore, G. M., DeLano, W. L., Gros, P., Grosse-Kunstleve, R. W., Jiang, J. S., Kuszewski, J., Nilges, M., Pannu, N. S., Read, R. J., Rice, L. M., Simonson, T., and Warren, G. L. (1998) Crystallography & NMR system: A new software suite for macromolecular structure determination, *Acta Crystallogr., Sect. D Biol. Crystallogr. 54* (Part 5), 905−921.
47. Rozek, A., Sparrow, J. T., Weisgraber, K. H., and Cushley, R. J. (1999) Conformation of human apolipoprotein C−I in a lipid-mimetic environment determined by CD and NMR spectroscopy, *Biochemistry 38*, 14475−14484.
48. Storjohann, R., Rozek, A., Sparrow, J. T., and Cushley, R. J. (2000) Structure of a biologically active fragment of human serum apolipoprotein C-II in the presence of sodium dodecyl sulfate and dodecylphosphocholine, *Biochim. Biophys. Acta 1486*, 253−264.
49. Ohman, A., Lycksell, P. O., and Graslund, A. (1993) A refined three-dimensional solution structure of a carboxy terminal fragment of apolipoprotein CII, *Eur. Biophys. J. 22*, 351−357.
50. Cheng, Q., Blackett, P., Jackson, K. W., McConathy, W. J., and Wang, C. S. (1990) C-terminal domain of apolipoprotein CII as both activator and competitive inhibitor of lipoprotein lipase, *Biochem. J. 269*, 403−407.
51. McIlhargey, T. L., Yang, Y., Wong, H., and Hill, J. S. (2003) Identification of a lipoprotein lipase cofactor-binding site by chemical cross-linking and transfer of apolipoprotein C-II-responsive lipolysis from lipoprotein lipase to hepatic lipase, *J. Biol. Chem. 278*, 23027−23035.
52. Hill, J. S., Yang, D., Nikazy, J., Curtiss, L. K., Sparrow, J. T., and Wong, H. (1998) Subdomain chimeras of hepatic lipase and lipoprotein lipase. Localization of heparin and cofactor binding, *J. Biol. Chem. 273*, 30979−30984.
53. Shen, Y., Lindberg, A., and Olivecrona, G. (2000) Apolipoprotein CII from rainbow trout (*Oncorhynchus mykiss*) is functionally active but structurally very different from mammalian apolipoprotein CII, *Gene 254*, 189−198.
54. Shen, Y., Lookene, A., Nilsson, S., and Olivecrona, G. (2002) Functional analyses of human apolipoprotein CII by site-directed mutagenesis: identification of residues important for activation of lipoprotein lipase, *J. Biol. Chem. 277*, 4334−4342.
55. MacPhee, C. E. (1999) The Specificity of Lipid−Protein Interactions, Ph.D. Thesis, The Russell Grimwade School of Biochemistry and Molecular Biology, University of Melbourne, Melbourne, Australia.
56. Razzaghi, H., Day, B. W., McClure, R. J., and Kamboh, M. I. (2001) Structure−function analysis of D9N and N291S mutations in human lipoprotein lipase using molecular modelling, *J. Mol. Graphics Modell. 19*, 487−494, 587−590.

BI049817L